



Phosphonic acid-grafted mesostructured silica/Nafion hybrid membranes for fuel cell applications

Jorphin Joseph^a, Chi-Yung Tseng^a, Bing-Joe Hwang^{a,b,*}

^a Nanoelectrochemistry Laboratory, Department of Chemical Engineering, National Taiwan University of Science and Technology, #43 Keelung Rd. Sec 4, Taipei 106, Taiwan, ROC

^b National Synchrotron Radiation Research Center, Hsinchu 300, Taiwan, ROC

ARTICLE INFO

Article history:

Received 21 July 2010

Received in revised form 27 August 2010

Accepted 27 August 2010

Available online 3 September 2010

Keywords:

Polymer electrolyte membrane

Nafion[®]

Composite

Mesoporous silica

Water retention

Proton conductivity

ABSTRACT

Highly conductive and hydration retentive mesoporous silica/Nafion and organically modified mesoporous silica/Nafion membranes are prepared by a surfactant templated sol-gel process involving Nafion solution and silica precursors. Spectroscopic analyses reveal that the *in situ* generation of a well-condensed silica network and organic ($-\text{PO}_3\text{H}_2$) functionalization of the inorganic segment are effectively achieved in the prepared membranes. The homogeneous dispersion of silica nanoparticles in the polymer matrix is apparent in electron micrographs. Structural analyses using small-angle X-ray scattering confirms the periodic short range structural order associated with these mesostructured hybrid membranes. These hybrid membranes exhibit an increased water uptake and an associated conductivity enhancement at 100% RH, compared to unmodified Nafion. More significantly, the functionalized silica/Nafion membranes show high proton conductivities at 80 °C and 50% RH, which is more than 6 times higher than that of Nafion. Thermogravimetric analysis, low temperature DSC studies and a comparison of activation energies (E_a) obtained from temperature-dependent conductivity plots of the membranes at different humidities, provide evidence for the better retention of water in the hybrid membranes compared to Nafion; thereby demonstrating the promising potential of these membranes to tolerate the variations in humidity at elevated temperatures.

© 2010 Elsevier B.V. All rights reserved.

1. Introduction

Polymer electrolyte fuel cells (PEMFCs) are the most promising renewable power-sources for emission-free vehicles and portable applications because of their high power densities, moderate operating temperatures and accordingly short start-up times [1]. Among the large variety of polymeric materials prepared for ion conductive fuel-cell membranes, DuPont's perfluorosulfonic acid polyelectrolyte Nafion[®] constitutes the present benchmark material regarding ion transport and longevity [2]. Despite the indisputable qualities of these polymer electrolytes with regard to proton conductivity, chemical and thermal stability, there are some disadvantages associated with these materials. The proton transport in these sulfonated polyelectrolytes is highly sensitive to dehydration at elevated temperatures and hydration imbalance due to water electro-osmotic drag. Under fuel cell operating conditions (50–80 °C), the changes in the humidity levels of the system

cause an increase in cell resistance and degradation of cell performance [3]. A strategy that has been suggested for improving the performances of Nafion[®] membranes during conditions of changing humidity is the incorporation of water retentive and inherently proton conductive fillers such as metal oxide particles (SiO_2 , TiO_2 , ZrO_2 , Al_2O_3) [4–13], heteropolyacids (phosphotungstic acid, silicotungstic acid) [14–16], zeolites (like mordenite) [17,18], layered silicates (like laponite) [19], zirconium phosphate [20,21] and phosphosilicate glass [22,23]. Although these composite membranes demonstrate adequate water uptakes and improved performance at elevated temperatures and low humidity conditions, the conductivities measured at high water activity is lower in these membranes compared to unmodified Nafion. This is because the presence of inorganic domains modifies the optimized ionic structure of Nafion and introduces higher tortuosity for the proton path in comparison to the unmodified Nafion. The distribution of particles and the interface between particles and Nafion polymeric matrix were also not satisfactory with these composite membranes. Poorly ordered, agglomerated dopants in the Nafion matrix (e.g. silica accumulation) and the formation of cracks on the surface were observed in some composite membranes [7,10], which are detrimental to the performance and durability of PEM fuel cells. However, the sol-gel method provides the advantage of generating

* Corresponding author at: Nanoelectrochemistry Laboratory, Department of Chemical Engineering, National Taiwan University of Science and Technology, #43 Keelung Rd. Sec 4, Taipei 106, Taiwan, ROC. Tel.: +886 2 27376624; fax: +886 2 27376644.

E-mail address: bjh@mail.ntust.edu.tw (B.-J. Hwang).

homogeneously dispersed silica particles with improved interaction between the metal oxide surface and Nafion polymer.

Recently, Pereira et al., have reported [24] the synthesis of Nafion-mesoporous silica hybrid membranes by the *in situ* generation of inorganic silica using surfactant assisted sol-gel process. This approach has the advantage of growing ordered mesoporous silica in the Nafion polymer without disrupting the proton transport pathways, while achieving great homogeneity at the micronic scale. In that contribution, sulfonic acid moieties were grafted on to mesoporous silica by post-oxidation reactions with a view to improve the conductivity. However, there is an increasing interest in using the phosphonic acid functions as an alternative for the sulfonic acid groups in fuel cell membranes operating in humidified environments and intermediate temperatures [25–33]. The main attractions of using $-\text{PO}_3\text{H}_2$ groups over $-\text{SO}_3\text{H}$ groups are due to the stability conferred in humid fuel cell environments and the water holding ability [34,35]. The greater aptitude of $-\text{PO}_3\text{H}$ groups for hydrogen-bonding can also reduce water swelling [36]. But a problem in relying completely on $-\text{PO}_3\text{H}_2$ groups for conductivity under humidified conditions is that the low room temperature conductivity of these systems may limit the start-up properties of the corresponding fuel cells. The relatively weak acidity of the phosphonic acid groups requires a moderate water uptake to maintain a reasonable conductivity. Hence it is anticipated that blending of commonly employed sulfonated materials with low contents of phosphonic acid functionalized phases can ensure the required high conductivities in the entire temperature range of fuel cell operation.

Here we report the synthesis and characterization of Nafion/phosphonic acid-grafted mesostructured silica hybrid membranes; in which the mesoporous silica network, embedded in the polymer and the $-\text{PO}_3\text{H}_2$ moieties, effectively retain water at low humidities, thereby giving materials with high conductivities. Moreover, the negative effects of inorganic domains with respect to proton conductivity at high water activity (as described earlier) are not observed in the present hybrid systems. In addition to the characterization of the new materials, we also present evidence for the improved water retention of the composite membranes.

2. Experimental

2.1. Materials

Nafion (DE 2021, DuPont, Wilmington, DE, USA) was obtained from Sigma-Aldrich, Co., as a 20 wt% solution in a mixture of lower aliphatic alcohols and water. Pluronic P123 (M.W. ~5800) was purchased from Aldrich Chemical Co. Tetraethoxysilane (TEOS, Aldrich) was used as the major silica source and diethylphosphonateethyltriethoxysilane (PETES, 95%, Gelest Inc.) was used to functionalize the inorganic network. Absolute ethanol (Aldrich) was used as the solvent. Hydrogen peroxide (30 wt%, Aldrich) and sulfuric acid (Fisher Scientific, UK) were used for the membrane post-treatments.

2.2. Nanocomposite membrane synthesis

The synthetic technique used in this work is based on the method proposed by Pereira et al. [24]. It is based on creating two individual homogeneous inorganic and organic solutions, which are then mixed and the solvent evaporated under carefully controlled conditions. The inorganic sol was prepared by mixing TEOS, P123 and ethanol in the molar ratios 1:0.003:16.3. For preparing functionalized silica/Nafion® composite membranes, 10 mol% of the TEOS in the above sol was replaced by organo-alkoxy silane, PETES. The inorganic sol containing surfactant was then added to a

stirred Nafion solution containing 20 wt% water. This solution was stirred at room temperature for 20 h, cast on to a clean glass plate and dried at 60 °C for 10 h. The hybrid membranes were then heated at 120 °C for 10 h to facilitate inorganic condensation and complete removal of the solvent. The resulting membranes were peeled off from the glass plate after immersing in water.

Crude membranes were post-treated as follows: (1) refluxing in boiling 3% H_2O_2 for 1 h to oxidize the inorganic impurities; (2) soaking in boiling deionized water for 1 h; (3) refluxing in boiling H_2SO_4 for 12 h to ensure complete protonation of Nafion, removal of the surfactant and hydrolysis of the phosphonate groups into PO_3H_2 groups (only in the case of functionalized composite membranes); (4) soaking in boiling deionized water for 2 h to remove excess acid.

In the present work, the starting compositions of TEOS or TEOS/PETES were fixed so as to obtain a total silica content of 10% in the composite membranes, assuming total conversion of silica precursors to silica. Nafion-silica membranes are designated as Nafion-TEOS. The functionalized membranes prepared from TEOS and PETES are named as Nafion-TEOS-PETES. For comparison, pure Nafion membranes were also prepared from 20 wt% solutions, by applying the same drying conditions.

2.3. Physico-chemical characterization

ATR-IR spectra of the membrane samples were collected on a Bio-Rad FTS-3500 equipped with an attenuated total reflection accessory using a ZnSe crystal. The spectra were collected as the average of 64 scans with a resolution of 4cm^{-1} over the range $4000\text{--}400\text{cm}^{-1}$. The solid-state NMR spectra were recorded on a Varian Infinity^{plus}-500 NMR spectrometer operating at a frequency of 99.035 MHz for the ^{29}Si nucleus and 201 MHz for ^{31}P nucleus using magic angle spinning technique. The chemical shifts are given with reference to tetramethylsilane. The cryogenically fractured membranes were examined with a scanning electron microscope (Jeol Model JSM6700 FE-SEM) coupled with a probe for energy-dispersive scanning (EDX) to study the morphology and elemental composition. A Philips/FEI TecnaiG20 transmission electron microscope (TEM) operating at 110 kV was also used to examine the hybrid morphology. The sample preparation involved embedding membranes in an EponTM-Araldite mixture followed by ultramicrotomy with a diamond knife to obtain thin sections which were placed on copper grids for TEM analysis. Small-angle X-ray scattering (SAXS) experiments were performed using the BL23A SWAXS instrument at National Synchrotron Radiation Research Center (NSRRC), Taiwan. The incident wavelength was $\lambda = 1.24\text{Å}$, and the sample to detector distance was varied so as to obtain an angular range of $0.006 < q < 0.3\text{Å}^{-1}$ with $q = 4\pi\lambda^{-1}\sin\theta$. For the measurement, the membranes were sealed in an air-tight-cell with Kapton windows. The SAXS data were corrected for transmission and background, and averaged as a function of scattering vector q . Thermogravimetric analysis under a N_2 atmosphere was used to determine the thermal stability of the membranes, and the status of the water (i.e. free water or bound water) in the membranes. Weight loss and derivative weight loss curves were obtained on a high-resolution Perkin Elmer Pyres1 instrument. All the hydrated membrane samples were nominally dried at 80 °C for one day before thermal analysis. The samples (~10 mg) were heated in nitrogen from room temperature to 800 °C with a heating rate of 10°Cmin^{-1} .

2.4. Water uptake, ion-exchange capacity and state of water

Water uptake (WU) was measured at room temperature. The samples were dried at 100 °C under vacuum for 12 h and then weighed (W_{dry}). These dried membranes were then immersed in

deionized water for 24 h and the fully hydrated membranes were weighed again (W_{wet}). The water uptake in percentage units was determined from the weight difference between wet and dry membranes using the following equation:

$$WU = \frac{W_{\text{wet}} - W_{\text{dry}}}{W_{\text{wet}}} \times 100$$

The ion-exchange capacity (IEC) of the composite membranes was determined by an acid–base titration. The membranes were dried under vacuum at 80 °C for 24 h followed by soaking in 1.0 M NaCl solution overnight. The salt solution (50 ml) was then titrated with 0.01 M NaOH using phenolphthalein indicator. The volume of NaOH consumed and the dry weight of the membranes were used to calculate the IEC. The titration was repeated for concordant values. Calorimetry experiments were performed by using differential scanning calorimeter from TA instruments (Model Q100) which was equipped with a refrigerated cooling unit for controlled cooling and sub-ambient temperature operation. A constant furnace atmosphere was maintained with a house nitrogen purge. The samples were first equilibrated in liquid water at room temperature for approximately 24 h. Excess water on the samples was gently wiped off before the samples were placed in hermetic aluminium pans, which were quickly sealed and weighed. During analysis, the samples were first cooled from 25 to –100 °C, held isothermally for 1 min, and then heated to 100 °C at a scan rate 5 °C min⁻¹. The amount of freezing water in the samples was calculated by integrating the peak area of the melt endotherm and comparing the value with the heat of fusion of ice.

2.5. Proton conductivity

Through-plane proton conductivity (σ) of the membranes was measured using an electrochemical impedance spectroscopy technique over the frequency range of 1 Hz–10⁷ Hz. Impedance data were acquired using a Solartron 1260 frequency response analyzer by applying a sinusoidal voltage of 10 mV amplitude. Z plot/Z view software was used to set the measurement parameters and to analyze the data. For the measurement, the membrane samples were placed between two stainless steel electrodes mounted on Teflon blocks. Conductivity measurements under fully hydrated conditions were performed by immersing the cell in deionized water at various temperatures. For measuring the conductivity as a function of temperature and relative humidity (RH), the cell was placed in a thermo-controlled humidity chamber (DENG YNG-DE80) and the membranes were conditioned at a set temperature and RH for about 6 h to obtain a steady value of resistance. The proton conductivity (σ) was then calculated using the following equation:

$$\sigma = l/RA$$

where l is the membrane thickness measured at ambient temperature and humidity, A is the electrode contact area and R is the bulk membrane resistance. For the measurements in liquid water, the swollen membrane thickness was used in the calculation of σ .

3. Results and discussion

3.1. Structural characterization by spectroscopic analysis

FTIR-ATR spectra of Nafion–TEOS membranes show characteristic bands of condensed silica [37] at 451 cm⁻¹ (associated with network Si–O–Si symmetric bending), 804 cm⁻¹ (symmetric Si–O–Si stretching of SiO₄ tetrahedra) and 1090 cm⁻¹ (asymmetric Si–O–Si stretching) (Fig. 1). Although this technique can give information about the presence and nature of Si–OH groups in the material [38], no peaks were detected around 930 cm⁻¹ (Si–OH

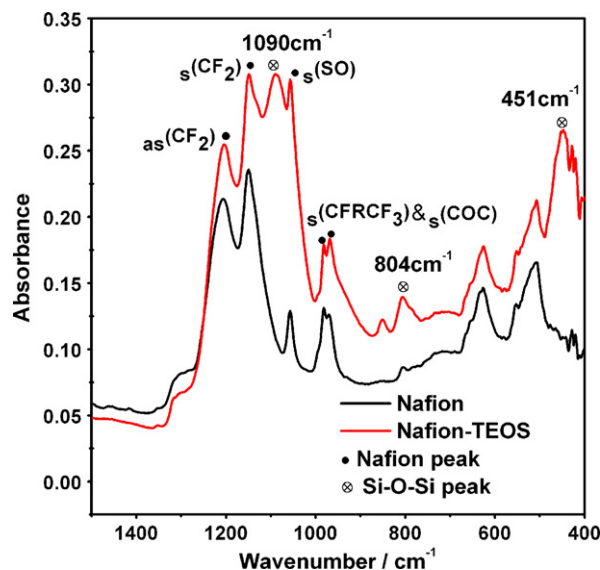


Fig. 1. FTIR spectra of recast Nafion and Nafion–silica hybrid membranes.

stretching) and the intensity of O–H bands, detected in the region 3800–2800 cm⁻¹, was very weak. This can be due to a significant degree of silanol condensation achieved in the composite membranes, which results in highly interconnected cross-linked Si–O–Si networks. Compared to a previous report [24] on the synthesis and characterization of mesostructured hybrid silica–Nafion membranes, the inorganic network seems to be more condensed in our case. The strong acid treatment conducted during membrane post-treatment might have facilitated the condensation reaction of residual silanol groups in the silica matrix.

To gather more information about the silicon environment and the extent of organic functionalization of the embedded inorganic phase, solid-state ²⁹Si MAS NMR spectra of the composite membranes were obtained. The Nafion–TEOS sample displaying Q₄ (–114.8 ppm) and Q₃ (–105 ppm) resonances (Fig. 2a), established that the *in situ* sol–gel reaction had occurred to form a well-condensed silica network inside the Nafion matrix. This spectrum is deconvoluted and the positions, widths and intensities of the lines attributed to the various Q_{*n*} groups are summarized in a table (Supplementary information). Although the lower signal-to-noise ratio, due to low contents of silica in the samples, does not allow strict quantification, the overall degree of silica condensation was determined (by approximation) as being ~94%. Such a high degree of silica condensation is highly desired as it has been reported [39] that incomplete hydrolysis of TEOS may leave residual ethyl groups on the surface of silica, which not only reduce the amount of water absorbed by silica but also blocks the pathway of proton transport in Nafion/silica membranes. The ²⁹Si NMR spectrum of functionalized silica/Nafion (inset Fig. 2a) shows the Q and T resonances contributed, respectively, by TEOS and PETES. The T resonance peaks appearing additionally in the spectrum indicate the incorporation of phosphonic acid functionalized silica in the inorganic network. Table 1 summarizes the chemical shifts obtained for various silicate structures, which are close to the corresponding

Table 1

Chemical shifts of different silica specie obtained from ²⁹Si NMR for Nafion–TEOS and Nafion–TEOS–PETES membranes.

	T ₁	T ₂	T ₃	Q ₃	Q ₄
Chemical shifts (ppm) for					
Nafion–TEOS				–105.0	–114.8
Nafion–TEOS–PETES	–47.7	–57.9	–64.7	–101.5	–111.7

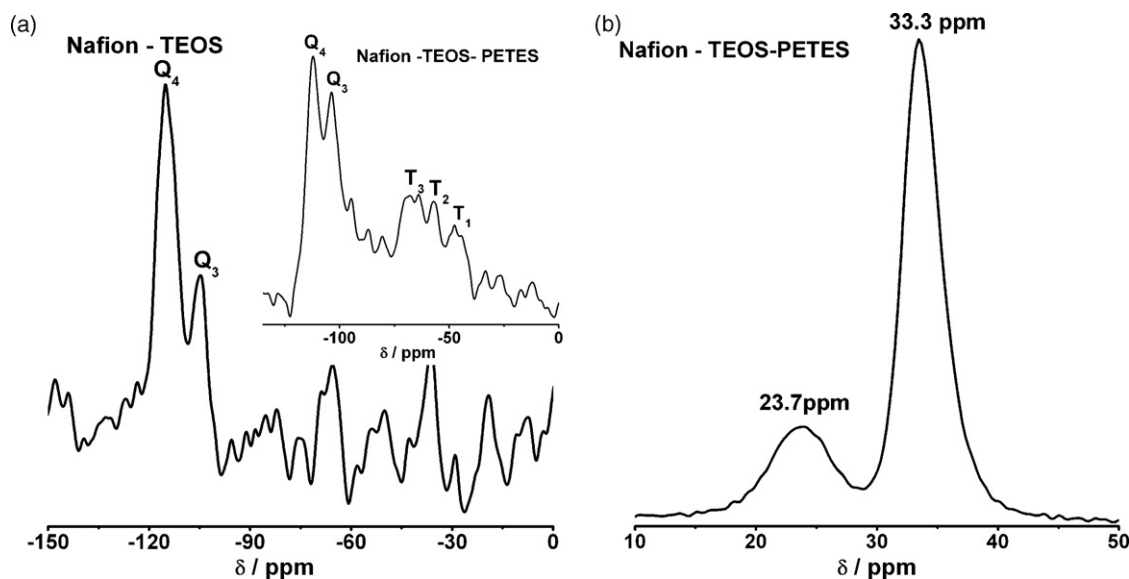


Fig. 2. (a) ^{29}Si MAS NMR spectra of Nafion–TEOS membrane and Nafion–TEOS–PETES membrane (inset) and (b) ^{31}P CPMAS NMR spectra of Nafion–TEOS–PETES membranes.

data reported in the literature [40]. ^{31}P NMR spectra of the samples were acquired (Fig. 2b) to verify the nature of the organic modifications to the membranes. The extremely strong peak at $\delta = 33.3$ ppm is attributed to $-\text{PO}_3\text{H}_2$ groups grafted on aliphatic chains via C–P bonds [41]. The ^{31}P resonance around ca. 23.7 ppm with one fifth the intensity of the resonance at 33.3 ppm is attributed to phosphonic acid moieties engaged in H-bonding interactions with the polymer or surface hydroxyl groups of silica. Aliev et al. [42] also have observed such trace peaks due to surface interactions between the phosphonic acid/phosphonate groups and the silica framework in ^{31}P spectra of sol–gel derived, phosphonic acid functionalized porous silica materials.

3.2. Morphology and nanostructure evaluation

The morphological features of the prepared membranes were examined using electron micrographs of the membranes. As illustrated in Fig. 3b, a fine homogeneous dispersion of the inorganic phase was observed throughout the polymer structure in the electron micrographs of the Nafion–TEOS composite membranes. Here, the surfactant assisted sol–gel synthesis has facilitated the condensation of sol–gel reactants without micronic segregation of silica phase. Such uniform dispersion of silica nanoparticles can improve the thermal and mechanical properties of the composite membranes [23] and their high surface area can facilitate proton hopping [43]. Although no surface defects were detected with the cast membranes, their surfaces were relatively rougher (Fig. 3a and b) compared to the surfaces of the melt-extruded commercial membranes. This may be due to the fast drying conditions applied during membrane casting. The TEM image of the composite membranes

(Fig. 3c) corresponds quite well with the SEM image (Fig. 3b). It has been reported [7] that Nafion/silica membranes containing higher contents of silica show asymmetric dispersion of silica domains and formation of cracks on the silica rich surface. But the atomic composition analysis by energy dispersive X-ray (EDX) (see Supporting information) showed the same intensity ratios on the surface and through the cross-section of the composite membranes. The Si/S weight ratio was found to be approximately 1.2 corresponding to a silica loading of 7.3%, a little less than the theoretically expected silica content (10%).

The nanostructure and morphology analysis of Nafion and the hybrid membranes have been conducted using SAXS. The clustering of ionic groups in Nafion is usually indicated by the existence of a scattering maximum at $q \sim 0.11 \text{ \AA}^{-1}$ [44] or $q \sim 0.13 \text{ \AA}^{-1}$ [45], often called as “ionomer peak” in small angle X-ray scattering (SAXS). The crystallites in the fluorocarbon matrix give rise to another prominent feature in the SAXS patterns of Nafion 117 which is commonly termed as ‘matrix knee’. This broad shoulder peak appears at $q < 0.05 \text{ \AA}^{-1}$ and it corresponds to an intercrystalline repeat length of 16–18 nm [46,47]. In the present study, the SAXS profiles obtained for pre-dried, unmodified Nafion clearly show the ionomer peak centered around $q \sim 0.14 \text{ \AA}^{-1}$ and a broad peak due to the crystallites at around $q \sim 0.05 \text{ \AA}^{-1}$ (Fig. 4). Although the ion cluster size in the Nafion polymer network depends on the hydration levels of the polymer, it has been reported [48] that ionic clusters exist even in dry Nafion membranes. For the dehydrated samples, the cluster size may be small with a small number of ionic SO_3H groups in each cluster and a small characteristic separation. A small shift of ionomer peak to higher q values observed in the present study as compared to the previ-

Table 2
Comparison of the characteristics of Nafion, silica/Nafion and functionalized silica/Nafion membranes.

Membrane	IEC mmol g^{-1}	Water uptake (wt%)	Bound water content (wt%)	$^a\sigma_{80}$ at 100%RH S cm^{-1}	$^b\sigma_{80}$ at 50% RH S cm^{-1}	cE_a at 100% RH kJ mol^{-1}	dE_a at 30% RH kJ mol^{-1}
Recast Nafion	0.89	14.9%	7.6%	0.080 ± 0.003 (68 μm)	0.008 ± 0.002 (61 μm)	13.5	19.3
Nafion–TEOS	0.84	18.5%	12.4%	0.089 ± 0.002 (88 μm)	0.014 ± 0.002 (74 μm)	13.6	16.8
Nafion–TEOS–PETES	0.92	24.9%	16.3%	0.152 ± 0.004 (91 μm)	0.049 ± 0.005 (74 μm)	13.6	14.5

^a Proton conductivity measured in liquid water at 80 °C.

^b Proton conductivity measured at 50% RH and 80 °C.

^c Activation energy measured at 100% RH in the temperature range 30–70 °C.

^d Activation energy measured at 30% RH in the temperature range 40–80 °C.

^e Thicknesses of the membranes used for conductivity measurements are given in parentheses.

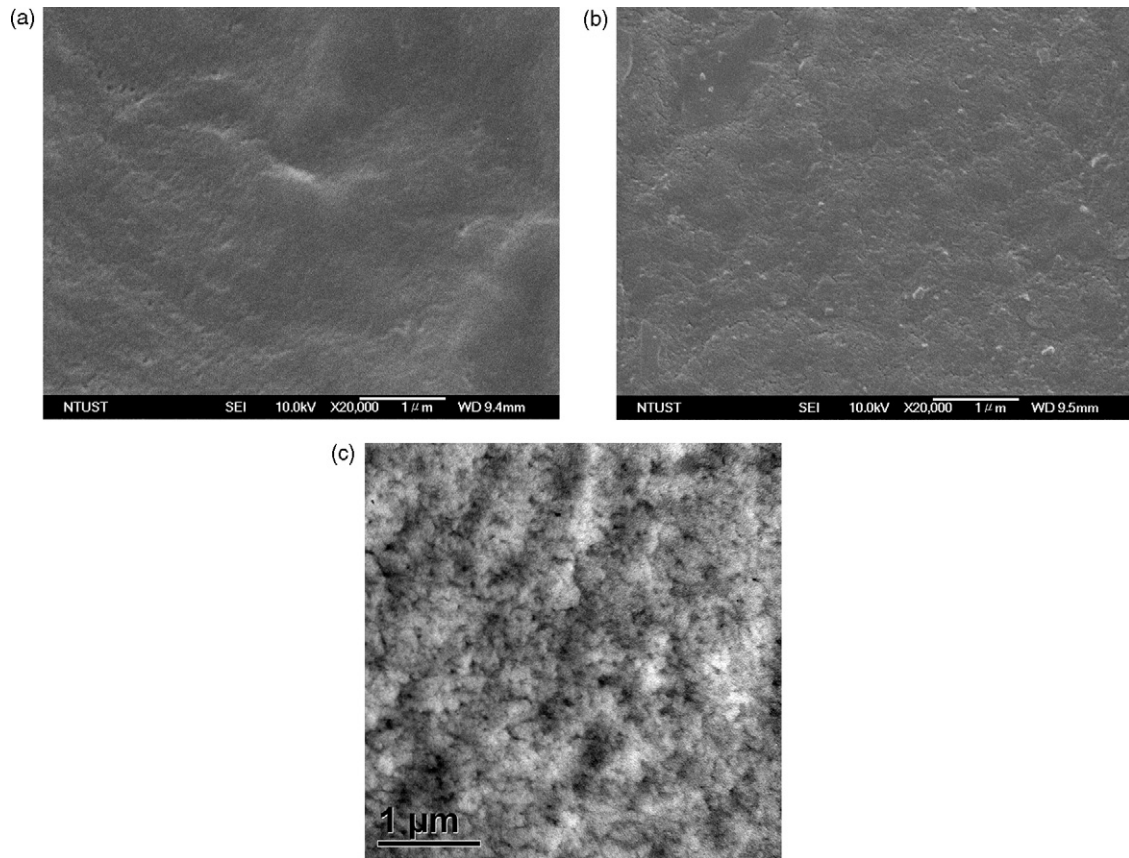


Fig. 3. (a) SEM images of recast Nafion, (b) Nafion-silica membranes and (c) TEM micrograph of Nafion-TEOS membrane showing silica dispersion within the polymer.

ous reports may be due to this effect. In a previous study [49], Kim et al. also observed ionomer peaks at $q \sim 0.14 \text{ \AA}^{-1}$ for vacuum dried Nafion 117 membranes. Interestingly, the composite membranes show a shift in the ionomer peak position to larger q values, at slightly less intensity than the Nafion peak. The higher q values obtained for the composite membranes, again, indicate that either the number density of ionic clusters increases or their clus-

ter size decreases in these systems, resulting in the reduction of the center-to-center cluster distance. In addition to the shift in ionomer peak, the SAXS patterns of surfactant-extracted composite membranes reveal the presence of mesoporous silica embedded in the polymer. Broad and intense Bragg peaks can be observed for all composite membranes with a characteristic d-spacing of about 11 nm. The d-spacing obtained is characteristic of mesostructured silica developed using P123 copolymer template [50]. A single diffraction peak in the SAXS pattern with no higher order Bragg peaks reveal that the pore organization does not exhibit mesoscopic order. This finding is similar to what is observed for materials exhibiting supramolecularly templated disordered mesoporosity [51,52].

3.3. Water uptake, state of water and thermal stability analysis

All hybrid membranes exhibit higher water uptake than unmodified cast Nafion (Table 2). The recast Nafion shows a water uptake of 14.9% whereas silica/Nafion and functionalized silica/Nafion membranes show higher uptake with 18.5% and 24.9%, respectively. Although slightly a higher thickness expansion was observed for the prepared hybrid membranes (Table 3), due to higher water contents associated with these membranes, no noticeable changes

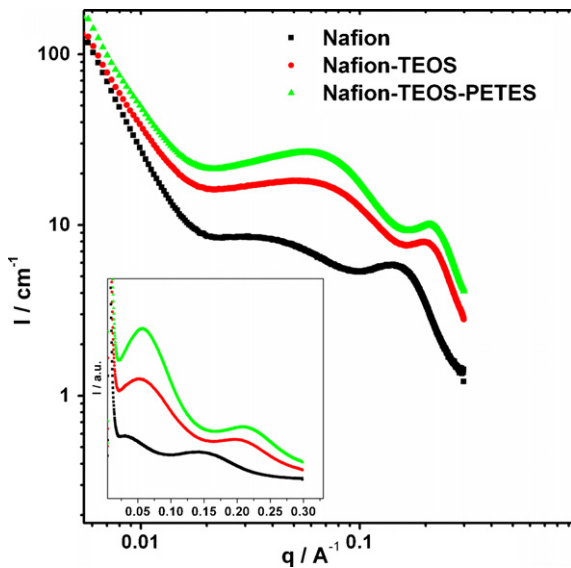


Fig. 4. Comparison of SAXS profiles of dry Nafion, Nafion-TEOS and Nafion-TEOS-PETES membranes in a $\log(I)$ versus $\log(q)$ plot. The inset shows the SAXS profiles obtained for the membranes in a linear plot of $I(q)$.

Table 3
Dimensional changes for recast Nafion and Nafion-hybrid membranes.

	Thickness (μm)		Thickness expansion (%)
	Dry	Wet	
Recast Nafion	60	72	20
Nafion-TEOS	74	90	22
Nafion-TEOS-PETES	76	93	22

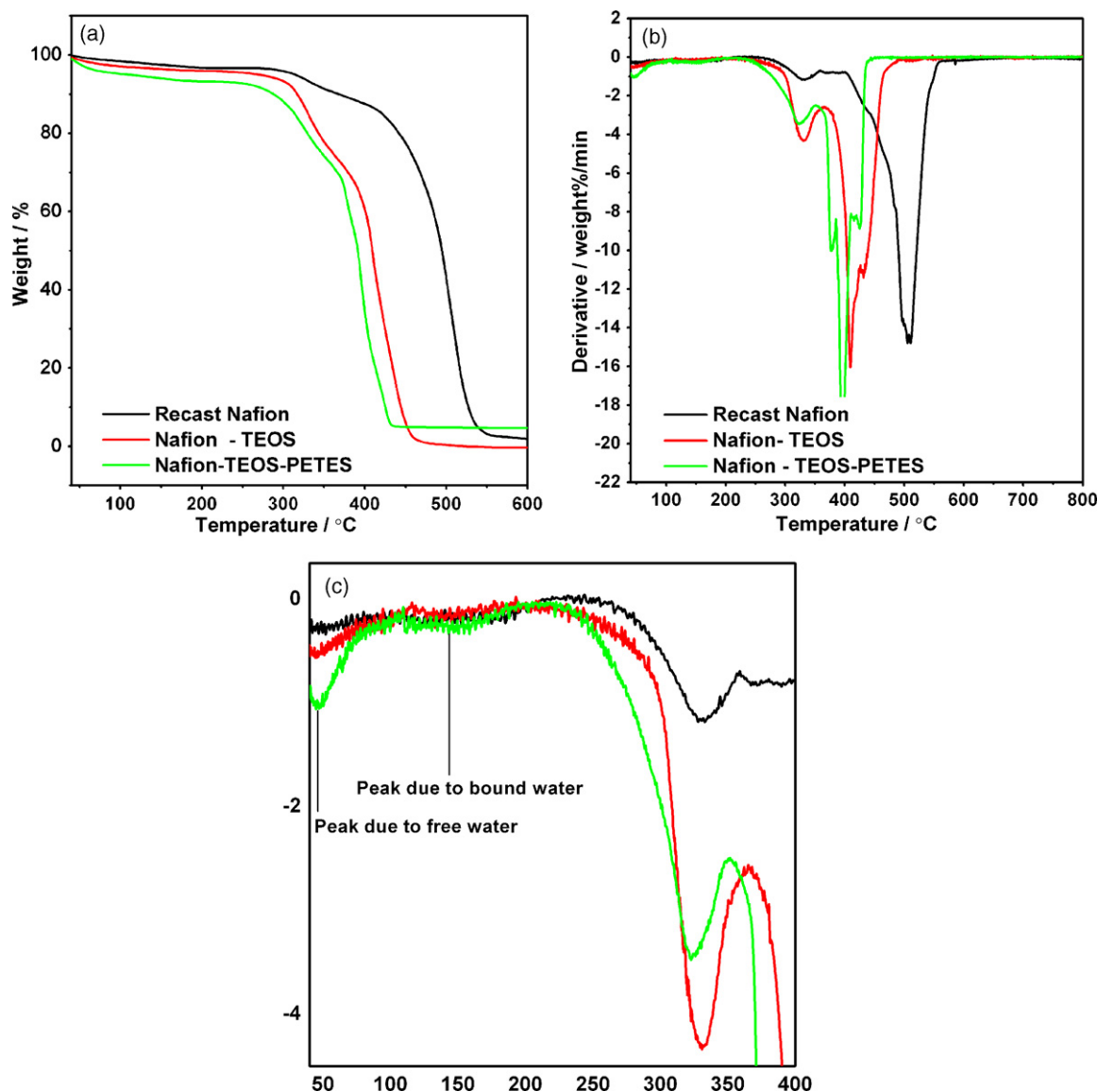


Fig. 5. (a) TGA thermograms, associated (b) derivative curves and (c) scale-expanded derivative curves of Nafion, Nafion-TEOS and Nafion-TEOS-PETES membranes.

were observed with regard to the mechanical properties of the membranes. TGA results also clearly demonstrate that the incorporation of the inorganic phase enhances the water content of the samples significantly. This can be ascribed to the presence of hydrophilic silica which holds water by hydrogen bonding. The thermograms for the nominally dried unmodified Nafion and those for the hybrid membranes are shown in Fig. 5a. The thermal decompositions of these membranes can be divided into three steps: dehydration, desulfonation and thermo-oxidation of the CF_2 backbone. The early weight losses below the decomposition temperature have to be attributed to the loss of absorbed water from the samples. Both Nafion and Nafion-hybrid membranes show the loss of residual water in two stages. The first peak in DTA (Fig. 5b) below 100°C corresponds to very loosely bound water within the membranes and the broad peak afterwards corresponds to strongly bound water embedded in the ionomeric cluster/mesoporous structure. The broad endotherm in the temperature range $100\text{--}200^\circ\text{C}$ corresponds to dehydration by the loss of strongly retained water in these membranes. Functionalized silica/Nafion membranes show high contents of strongly

bound water (Fig. 5c). This is in close agreement with the previous reports in which mesoscopically ordered silica [53] or organosilica [54] frameworks synthesized by the use of surfactants as structure-directing agents, effectively retain the molecular water absorbed in the inner pore surfaces at elevated temperatures. The thermal degradation corresponding to the decomposition of sulfonic acid groups occurs at around 300°C in all the membranes; however, the subsequent decomposition in hybrid membranes is found to occur at lower temperatures than in the unmodified Nafion membranes. Mauritz and coworkers also found [55] that the decomposition of Nafion was extended to higher temperatures as compared with that of Nafion containing 13.4% silica. The intervening silica fragments in the hybrid membranes do not allow physical cross-linking provided by the side-chain aggregation. Hence, once the inorganic cages are degraded, thermal decomposition occurs more abruptly in the hybrid membranes compared to unmodified Nafion. It is also possible that the volatile compounds such as SiF_4 formed during heating catalyzes subsequent degradation. For the phosphonic acid functionalized silica/Nafion hybrid membranes, an early start of primary

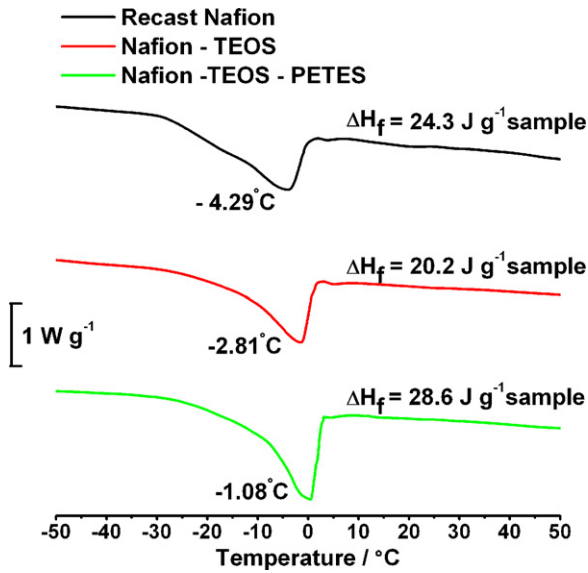


Fig. 6. DSC thermograms of hydrated recast Nafion and Nafion-silica hybrid membranes (−50 °C to 50 °C).

degradation and an additional endothermic peak are observed. The condensation of PO_3H_2 groups (starting from 220 °C) and decomposition of phosphonic acid group-bearing side chains are responsible for these thermal degradations. The above results suggest that the new membranes have good thermal stability up to 220 °C.

The local environment of water in the membranes can be identified from the temperature at which it freezes in the membranes. Fig. 6 shows DSC thermograms of the membranes in the temperature range −50–50 °C. The melting temperature of water in fully hydrated Nafion is −4.29 °C, whereas the same transition occurs at −2.81 °C and −1.08 °C, respectively, for fully hydrated Nafion-TEOS and Nafion-TEOS-PETES membranes. The shift of melting transitions to lower temperatures (decrease in the colligative property) can be due to the increased water uptake of the hybrid membranes which reduces the local acid concentration [56]. Low temperature DSC was used to quantify and elucidate the different types of water in Nafion and Nafion-composite membranes (Table 2).

The composite membranes show higher contents of nonfreezing water as compared to unmodified Nafion. This can be due to the higher degree of confinement that absorbed water experiences in the composite membranes. But in the light of a recent article [57], which raises a cautionary note on the quantitative use of this thermodynamic data for describing the microenvironments of water within the membrane, the discussion based on DSC data has been restricted to compliment our other observations. The water uptake, thermogravimetric analysis and DSC results of the prepared membranes suggest that a significant amount of the strongly retained water is embedded in the composite membranes as compared to Nafion. Such an increase in water content can decrease the restraining forces on protons (exerted by the counter ions) and facilitate ‘proton hopping’ for high proton conductivity.

3.4. Proton conductivity

Proton hopping and vehicular diffusion are believed to be the predominant modes of proton conduction in the ionomer membranes [58,59]. An increase in temperature increases conductivity as it strongly affects both mechanisms: hopping as well as diffusion becomes faster. Notably, the conductivity also increases with the dilution of charge carriers (increasing water content of the samples). An increase in conductivity, when increasing water content of the membranes is caused by an increase in proton mobility. But in the PEMFC operating range (50–80 °C) conductivity increases only about 20% for a temperature increase by 10 °C whereas it increases nearly by an order of magnitude with increasing water content. Therefore, water content and the related proton mobility are identified as the key parameters affecting membrane conductivity. The proton conductivities of recast Nafion and the Nafion hybrids measured at different relative humidity (RH) and 80 °C are shown in Table 2. At 100% RH and 80 °C, Nafion/silica membrane shows a proton conductivity of 0.089 S cm^{-1} , compared to 0.080 S cm^{-1} for recast Nafion 117. It has been reported that in the production of hybrid silica-Nafion membranes, the presence of inorganic siloxane domains could interfere with the structure of the ionic clusters and accordingly reduce the proton conductivity measured at high water activity [23]. Nevertheless the presence of mesoporous silica has not disrupted the proton transport pathway in the present study. Moreover, the incorporation of dispersed, nanostructured, hygroscopic silica has slightly improved the proton conductivity of

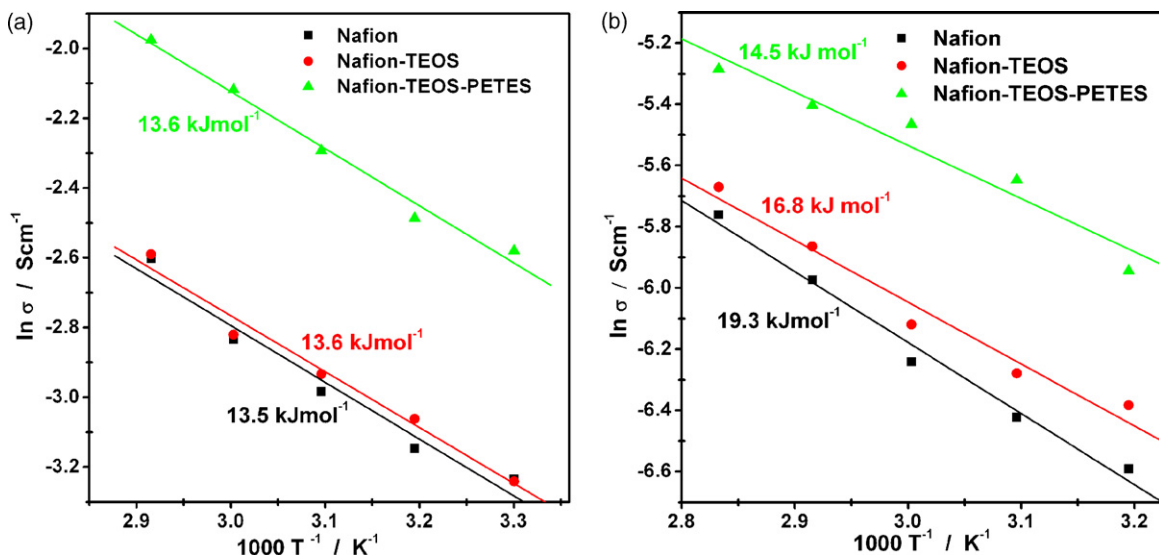


Fig. 7. Arrhenius plots for the proton conductivity of the membranes as a function of temperature, at: (a) 100% RH and (b) 30% RH.

Nafion. However, a much improved performance ($\sigma = 0.152 \text{ S cm}^{-1}$) is observed with the functionalized silica/Nafion membranes at 80 °C and 100% RH, possibly due to a combination of high water uptake and increased charge carrier concentration.

For practical applications, the performance of the membranes at low humidity is crucially important: this aspect of the membrane's response was examined by comparing the conductivities of the composite membranes with Nafion membranes at RH = 50%. Under low humidity conditions, the proton conductivities of all the membranes are significantly lower (Table 2) because all these materials rely on water for proton transport. However, the hybrid membranes show higher conductivity in comparison to those of Nafion at 50% RH. The increased conductivity at low humidity suggests that the Nafion/silica hybrid has better water retention properties than recast Nafion. The growth of phosphonated mesoporous silica in Nafion membrane yields a material with much improved proton conduction ($\sigma = 0.049 \pm 0.005 \text{ S cm}^{-1}$) at low humidity conditions.

The temperature-dependent conductivities of the prepared membranes were plotted at RH = 100% and 30% (Fig. 7a and b). The activation energies (E_a) for proton conduction were obtained from these Arrhenius plots (Table 2). Under fully humidified conditions, the activation energy for Nafion 117 was calculated to be 13.5 kJ mol^{-1} , which is the same as the published data in the temperature range 20–90 °C [44]. The activation energies obtained for hybrid membranes are very close to those of recast Nafion indicating that all the prepared membranes have similar proton conduction pathways under these conditions. The water present in the membranes might be acting as a well connected network for proton hopping. But the situation is different at 30% RH, i.e. when the water content of Nafion is diminished significantly. In this case the activation energy for Nafion increases to 19.3 kJ mol^{-1} , indicating a change in the conductivity mechanism; but, for functionalized hybrid membranes, E_a does not change too much because water is effectively retained in these membranes, favoring vehicular diffusion of protons [24,60].

4. Conclusion

Novel mesostructured silica/Nafion and mesostructured phosphonated silica/Nafion hybrid membranes have been prepared using a surfactant templated sol-gel process. In contrast to conventional Nafion/silica composites, the growth of mesoporous inorganic network was accomplished without disrupting the proton transport pathways resulting in proton conductivities higher than those of pristine Nafion over a range of temperatures and relative humidities. More significantly, phosphonate functionalized silica/Nafion membranes display conductivities almost 6 times higher than that of unmodified Nafion at high temperatures and low humidity. The porous silica network and the $-\text{PO}_3\text{H}_2$ functionalities were identified as playing a dominant role in retaining water under low humidity, leading to high conductivity. This work demonstrates the promising potential of such modified Nafion composites for applications in high temperature PEMFCs.

Acknowledgments

The authors gratefully acknowledge financial support from the National Science Council, facilities from National Taiwan University of Science and Technology and the National Synchrotron Radiation Research Center, Taiwan. The authors would also like to acknowledge the assistance given by Dr. John Rick towards the completion of this manuscript. J. J. gratefully acknowledges a Taiwan Scholarship given by the Ministry of Education, Republic of China (Taiwan).

Appendix A. Supplementary data

Supplementary data associated with this article can be found, in the online version, at doi:10.1016/j.jpowsour.2010.08.090.

References

- [1] L. Carrette, K.A. Friedrich, U. Stimming, *Fuel Cells* 1 (2001) 5–39.
- [2] Q. Li, R. He, J.O. Jensen, N.J. Bjerrum, *Chem. Mater.* 15 (2003) 4896–4915.
- [3] R.J. Bellows, M.Y. Lin, M. Arif, A.K. Thompson, D. Jacobson, *J. Electrochem. Soc.* 146 (1999) 1099–1103.
- [4] Q. Deng, R.B. Moore, K.A. Mauritz, *Chem. Mater.* 7 (1995) 2259–2268.
- [5] M. Watanabe, H. Uchida, Y. Seki, M. Emori, P. Stonehart, *J. Electrochem. Soc.* 143 (1996) 3847–3852.
- [6] P.L. Antonucci, A.S. Arico, P. Creti, E. Ramunni, V. Antonucci, *Solid State Ionics* 125 (1999) 431–437.
- [7] N. Miyake, J.S. Wainright, R.F. Savinell, *J. Electrochem. Soc.* 148 (2001) 898–904.
- [8] N.H. Jalani, K. Dunn, R. Datta, *Electrochim. Acta* 51 (2003) 553–560.
- [9] K.T. Adjemian, R. Dominey, L. Krishnan, H. Ota, P. Majsztrik, T. Zhang, J. Mann, B. Kirby, L. Gatto, M.V. Simpson, J. Leahy, S. Srinivasan, J.B. Benziger, A.B. Bocarsly, *Chem. Mater.* 18 (2006) 2238–2248.
- [10] A.K. Sahu, G. Selvarani, S. Pitchumani, P. Sridhar, A.K. Shukla, *J. Electrochem. Soc.* 154 (2007) B123–132.
- [11] H.L. Tang, M. Pan, *J. Phys. Chem. C* 112 (2008) 11556–11568.
- [12] A. Sacca, I. Gatto, A. Carbone, R. Pedicini, E. Passalacqua, *J. Power Sources* 163 (2006) 47–51.
- [13] A.D. Epifanio, M.A. Navarra, F.C. Weise, B. Mecheri, J. Farrington, S. Licocchia, S. Greenbaum, *Chem. Mater.* 22 (2010) 813–821.
- [14] B. Tazi, O. Savadogo, *Electrochim. Acta* 45 (2000) 4329–4339.
- [15] V. Ramani, H.R. Kunz, J.M. Fenton, *J. Membr. Sci.* 232 (2004) 31–44.
- [16] Z.-G. Shao, H. Xu, M. Li, I.-M. Hsing, *Solid State Ionics* 177 (2006) 779–785.
- [17] S.-H. Kwak, T.-H. Yang, C.-S. Kim, K.H. Yoon, *Solid State Ionics* 160 (2003) 309–315.
- [18] D.-H. Son, R.K. Sharma, Y.G. Shul, H. Kim, *J. Power Sources* 165 (2007) 733–738.
- [19] P. Bebin, M. Caravanier, H. Galiano, *J. Membr. Sci.* 278 (2006) 35–42.
- [20] C. Yang, S. Srinivasan, A.B. Bocarsly, S. Tulyani, J.B. Benziger, *J. Membr. Sci.* 237 (2004) 145–161.
- [21] G. Alberti, M. Casciola, D. Capitani, A. Donnadio, R. Narducci, M. Pica, M. Sganappa, *Electrochim. Acta* 52 (2007) 8125–8132.
- [22] M. Aparicio, L.C. Klein, *J. Electrochem. Soc.* 152 (2005) A493–A496.
- [23] A.G. Kannan, N.R. Choudhuri, N.K. Dutta, *J. Membr. Sci.* 333 (2009) 50–58.
- [24] F. Pereira, K. Valle, P. Belleville, A. Morin, S. Lambert, C. Sanchez, *Chem. Mater.* 20 (2008) 1710–1718.
- [25] Y.Z. Meng, S.C. Tjong, A.S. Hay, S.J. Wang, *J. Polym. Sci. A: Polym. Chem.* 39 (2001) 3218–3226.
- [26] H.R. Allcock, M.A. Hofmann, C.M. Ambler, S.N. Lvov, X.Y. Zhou, E. Chalkova, J. Weston, *J. Membr. Sci.* 201 (2002) 47–54.
- [27] Y.M. Li, K. Hinokuma, *Solid State Ionics* 150 (2002) 309–315.
- [28] S. Yanagimachi, K. Kaneko, Y. Takeoka, M. Rikukawa, *Synthetic Met.* 135–136 (2003) 69–70.
- [29] M. Yamada, I. Honma, *Polymer* 46 (2005) 2986–2992.
- [30] E. Parcerro, R. Herrera, S.P. Nunes, *J. Membr. Sci.* 285 (2006) 206–213.
- [31] S. Li, Z. Zhou, H. Abernathy, M. Liu, W. Li, J. Ukai, K. Hase, M. Nakanishi, *J. Mater. Chem.* 16 (2006) 858–864.
- [32] A. Kaltbeitzel, S. Schauff, H. Steininger, B. Bingol, G. Brunklaus, W.H. Meyer, H.W. Spiess, *Solid State Ionics* 178 (2007) 469–474.
- [33] G. Brunklaus, S. Schauff, D. Markova, M. Klapper, K. Mullen, H.W. Spiess, *J. Phys. Chem. B* 113 (2009) 6674–6681.
- [34] M. Rikukawa, K. Sanui, *Prog. Polym. Sci.* 25 (2000) 1463–1502.
- [35] M. Schuster, T. Rager, A. Noda, K.D. Kreuer, J. Maier, *Fuel Cells* 3 (2005) 355–365.
- [36] T. Bock, H. Mohwald, R. Mulhaupt, *Macromol. Chem. Phys.* 208 (2007) 1324–1340.
- [37] A. Bertoluzza, C. Fagnano, M.A. Morelli, V. Gottardi, M. Guglielmi, *J. Non-cryst. Solids* 48 (1982) 117–128.
- [38] P. Innocenzi, *J. Non-cryst. Solids* 316 (2003) 309–319.
- [39] G. Ye, C.A. Hayden, G.R. Goward, *Macromolecules* 40 (2007) 1529–1537.
- [40] R.H. Glaser, G.L. Wilkes, C.E. Bronnimann, *J. Non-cryst. Solids* 113 (1989) 73–87.
- [41] W. Gao, L. Dickinson, C. Grozinger, F.G. Morin, L. Reven, *Langmuir* 12 (1996) 6429–6435.
- [42] A. Aliev, D.L. Ou, B. Ormsby, A.C. Sullivan, *J. Mater. Chem.* 10 (2000) 2758–2764.
- [43] V. Ramani, H.R. Kunz, J.M. Fenton, *J. Membr. Sci.* 266 (2005) 110–114.
- [44] J. Halim, F.N. Buchi, O. Hass, M. Stamm, G.G. Scherer, *Electrochim. Acta* 39 (1994) 1303–1307.
- [45] G. Gebel, *J. Lambard, Macromolecules* 30 (1997) 7914–7920.
- [46] E.J. Roche, M. Pineri, R. Duplessix, A.M. Levelut, *J. Polym. Sci. Polym. Phys. Ed.* 19 (1981) 1–11.
- [47] R.B. Moore, C.R. Martin, *Macromolecules* 21 (1988) 1334–1339.
- [48] B. Yang, A. Manthiram, *J. Power Sources* 153 (2006) 29–35.
- [49] J.-D. Kim, M. Ohnuma, C. Nishimura, T. Mori, A. Kucernak, *J. Electrochem. Soc.* 156 (2009) B729–B734.
- [50] D. Zhao, Q. Huo, J. Feng, B.F. Chmelka, G.D. Stucky, *J. Am. Chem. Soc.* 120 (1998) 6024–6036.
- [51] J.-L. Bliin, A. Leonard, Z.-Y. Yuan, L. Gigot, A. Vantomme, A.K. Cheetham, B.-L. Su, *Angew. Chem. Int. Ed.* 42 (2003) 2872–2875.

- [52] G.V.R. Rao, G.P. Lopez, J. Bravo, H. Pham, A.K. Datye, H. Xu, T.L. Ward, *Adv. Mater.* 18 (2002) 1301–1304.
- [53] H. Li, M. Nogami, *Adv. Mater.* 12 (2002) 912–914.
- [54] R. Marschall, J. Rathousky, M. Wark, *Chem. Mater.* 19 (2007) 6401–6407.
- [55] Q. Deng, C.A. Wilkie, R.B. Moore, K.A. Mauritz, *Polymer* 24 (1998) 5961–5972.
- [56] A. Siu, J. Schmeisser, S. Holdcroft, *J. Phys. Chem. B* 110 (2006) 6072–6080.
- [57] T.L. Kalapos, B. Decker, H.A. Every, H. Ghassemi, T.A. Zawodzinski Jr., *J. Power Sources* 172 (2007) 14–19.
- [58] K.D. Kreuer, *Solid State Ionics* 94 (1997) 55–62.
- [59] M. Eikerling, A.A. Kornyshev, A.M. Kuznetsov, J. Ulstrup, S. Walbran, *J. Phys. Chem. B* 105 (2001) 3646–3662.
- [60] K.D. Kreuer, *Chem. Mater.* 8 (1996) 610–641.